

Non-Markovian Dynamics of Open Quantum Gases

Tim Bode,^{1,2,*} Michael Kajan,¹ Francisco Meirinhos,¹ and Johann Kroha^{1,†}

¹*Physikalisches Institut and Bethe Center for Theoretical Physics,*

Universität Bonn, Nussallee 12, 53115 Bonn, Germany

²*Institute for Quantum Computing Analytics (PGI-12),*

Forschungszentrum Jülich, 52425 Jülich, Germany

We introduce an auxiliary-particle field theory to treat the non-Markovian dynamics of driven-dissipative quantum systems of the Jaynes-Cummings type. It assigns an individual quantum field to each reservoir state and provides an analytic, faithful representation of the coupled system-bath dynamics. We apply the method to a driven-dissipative photon Bose-Einstein condensate (BEC) coupled to a reservoir of dye molecules with electronic and vibronic excitations. The complete phase diagram of this system exhibits a hidden, non-Hermitian phase transition separating temporally oscillating from biexponentially decaying photon density correlations within the BEC. On one hand, this provides a qualitative distinction of the thermal photon BEC from a laser. On the other hand, it shows that one may continuously tune from the BEC to the lasing phase by circumventing a critical point. This auxiliary-particle method is generally applicable to the dynamics of open, non-Markovian quantum systems.

Experimental platforms coupling a set of photonic cavity modes to an ensemble of dye molecules, comprised of two-level systems (TLS) of electronic excitations and local vibrational degrees of freedom, are relevant for applications ranging from Bose-Einstein condensates (BEC) of photons [1–5], exciton polaritons [6, 7] and plasmonic lattices [8] to single-photon sources for quantum information [9]. Despite general non-equilibrium field theory being available [10], the non-equilibrium stationary states and dynamics of such open, driven-dissipative quantum gases are unexplored to a large extent. Recently, measurements of the second-order coherence in photon BECs [11, 12] have opened the door to a deeper understanding. In fact, the experiments revealed a hidden, complex structure in the temporal correlations which undergo a non-Hermitian phase transition as the system is driven away from equilibrium, while the spectral mode occupation still follows an equilibrium Bose-Einstein distribution.

As open quantum systems are driven far from equilibrium, reservoir frequency scales like the spectral substructure [13] and relaxation rates can no longer be considered fast compared to the photonic cavity loss and tunneling rates. In particular, in multiple coupled cavities [14], fast Josephson oscillations can approach the time scales of such reservoir processes. In these cases, quantum coherence and non-Markovian memory effects [9, 15] are expected to become important. The theoretical treatment of this non-Markovian regime is complicated by the vast number of reservoir degrees of freedom and the necessity of describing their full quantum dynamics (FQD). Direct numerical time-evolution methods are limited to rather small systems, and the extension to larger systems requires truncation of the quantum entanglement between the subsystems [16]. On the other hand, approximate techniques based on the Born-Markov approximation and rate equations (RE) [17–21], well established

for Markovian dynamics even in large systems, inherently cannot capture non-Markovian memory or quantum coherence effects. Standard field-theoretic techniques suitable for a large number of degrees of freedom, like the quantum Langevin approach [22], are hampered by the non-canonical statistics of the pseudospin operators involved in the electronic TLS dynamics, which have, for this reason, been approximated by bosons.

In this Letter, we develop a general field-theoretic technique based on an auxiliary-particle representation, which captures the non-canonical reservoir dynamics exactly, to describe a large class of coherent, light-matter coupled, open quantum systems such as the Holstein-Tavis-Cummings Hamiltonian or arbitrary TLS in a cavity, and generalize it to strong, time-dependent non-equilibrium. In this approach, an individual canonical quantum field is assigned to each matter state (electronic and vibronic molecule excitations), with the constraint that the system occupies exactly one of these states at any instance of time. Because of the canonical commutation relations, the auxiliary-field dynamics are amenable to standard field-theoretic techniques, and the exact confinement to the physical Hilbert space defined by the above-mentioned constraint is performed analytically as long as correlations between different molecules can be neglected. The auxiliary-particle method has been pioneered by Abrikosov [23] and Barnes [24, 25] and is successfully used [26–29] for strongly correlated electron systems like the Anderson impurity model [30]. The extension to stationary non-equilibrium has been developed in [31–34], and a more recent exposition for correlated electrons in time-dependent non-equilibrium can be found in [35]. Generalizing this to quantum optics, we discover an exceptional point in the dynamics of the second-order coherence for large losses, followed by a non-equilibrium decondensation phase transition indicated by critical slowing down. We demonstrate how non-Markovian effects

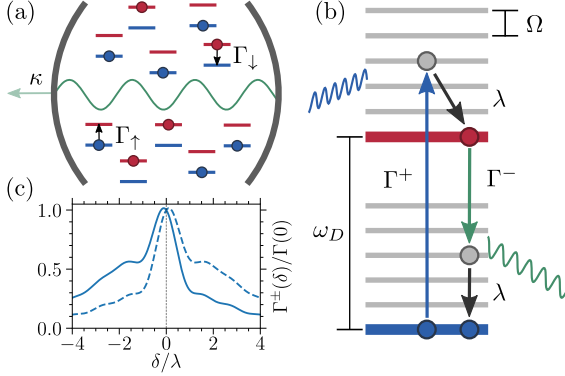


FIG. 1: (a) Sketch of the dye-filled microcavity. (b) A typical cycle of absorption (Γ^+) and emission (Γ^-) with intermediate vibrational relaxation (λ). (c) Steady-state absorption (dashed) and emission (solid) spectra $\Gamma^\pm(\delta)$ as computed from the photon self-energies (cf. Eq. (S.7) of [36]) for $\Omega/\lambda = 2$, $S = 0.25$, $\bar{n} = 0.25$, $\Gamma_\uparrow = \Gamma_\downarrow = 0$, and $\lambda\Gamma(0) = g^2 \cdot 1.298$.

become relevant in the strongly driven-dissipative regime.

Model and auxiliary-particle representation. – We consider a class of Hamiltonians of the form $H = H_0 + H_{\text{ep}} + H_{\text{JC}}$, where $H_0 = \sum_k \omega_k a_k^\dagger a_k + \sum_{m=1}^M \omega_D \sigma_m^z / 2 + \Omega b_m^\dagger b_m$ describes a set of cavity modes with dispersion ω_k , as well as M molecules comprised of an electronic TLS with splitting ω_D and a phonon mode Ω (the generalization to multiple phonon modes is straightforward). The Jaynes-Cummings (JC) coupling in the rotating-wave approximation reads $H_{\text{JC}} = g \sum_{k,m} (a_k \sigma_m^+ + a_k^\dagger \sigma_m^-)$. In these expressions, a_k^\dagger, b_m^\dagger are the creation operators for a photon or a phonon quantum, respectively, and σ_m^z, σ_m^\pm are Pauli operators describing the electron dynamics. Electron-phonon coupling results from the phononic-oscillator displacement $\hat{x}_m = b_m + b_m^\dagger$ depending on the electronic TLS state and reads $H_{\text{ep}} = \sum_m \Omega \sqrt{s} \sigma_m^z (b_m + b_m^\dagger)$.

A single molecule has quantum states $|\sigma, n\rangle$, where $\sigma = g, e$ refers to the electronic ground and excited state, respectively, and n denotes the vibrational state. For each of these states, we introduce auxiliary or pseudo-boson operators $d_{\sigma,n}, d_{\sigma,n}^\dagger$ with $[d_{\sigma,n}, d_{\sigma',n'}^\dagger] = \delta_{\sigma\sigma'}\delta_{nn'}$ defined by $d_{\sigma,n}^\dagger |{\text{vac}}\rangle = |\sigma, n\rangle$. The molecular operators may then be expressed as

$$b = \sum_{n=0}^{\infty} \sum_{\sigma=g,e} \sqrt{n+1} d_{\sigma,n}^\dagger d_{\sigma,n+1}, \quad (1)$$

$$\sigma^+ = \sum_{n=0}^{\infty} d_{e,n}^\dagger d_{g,n}, \quad \sigma^- = \sum_{n=0}^{\infty} d_{g,n}^\dagger d_{e,n},$$

where we have dropped the subscripts m . This representation is faithful within the Hilbert space spanned by the states $|\sigma, n\rangle$ (no product states of these), i.e., under the operator constraint that the total auxiliary particle number $\hat{Q} = \sum_{n=0}^{\infty} \sum_{\sigma} d_{\sigma,n}^\dagger d_{\sigma,n} = 1$. In the frame rotating with the electronic frequency ω_D , the Hamiltonian

for $M = 1$ thus reads

$$H = \sum_k \delta_k a_k^\dagger a_k + \sum_{n=0}^{\infty} \left[n\Omega (d_{e,n}^\dagger d_{e,n} + d_{g,n}^\dagger d_{g,n}) \right. \\ \left. + \Omega \sqrt{S(n+1)} (d_{e,n+1}^\dagger d_{e,n} - d_{g,n+1}^\dagger d_{g,n} + \text{h.c.}) \right. \\ \left. + g \sum_k (a_k^\dagger d_{g,n}^\dagger d_{e,n} + a_k d_{e,n}^\dagger d_{g,n}) \right], \quad (2)$$

where $\delta_k = \omega_k - \omega_D$ is the resonator detuning. We note in passing that in pseudo-boson representation, the molecular part of this Hamiltonian is quadratic. That is, the polaron transformation diagonalizing this part is straightforward and commutes with the constraint $\hat{Q} = 1$, but transforms the molecule-photon coupling into $\sum_{mn} \gamma_{mn} (a_k^\dagger d_{g,m}^\dagger d_{e,n} + \text{h.c.})$, where the coupling matrix γ_{mn} may be calculated analytically and is proportional to the Franck-Condon integrals. In the following, we will use the non-diagonal representation Eq. (2) for quantitative evaluations.

Hilbert-space projection. – The projector onto the physical $\hat{Q} = 1$ sector of Hilbert space can be represented as

$$\hat{P} = \lim_{\mu \rightarrow \infty} \hat{Q} e^{-\mu(\hat{Q}-1)} = \lim_{\zeta \rightarrow 0} \hat{Q} \zeta^{(\hat{Q}-1)}, \quad (3)$$

where the fugacity is $\zeta = \exp(-\mu)$, and the (dimensionless) chemical potential μ can be gauged time independent, because the Hamiltonian (2) conserves the auxiliary-particle number \hat{Q} . In this way, the $(\hat{Q} = 1)$ -projected partition function is obtained as

$$Z_{\hat{Q}=1} = \lim_{\zeta \rightarrow 0} \text{Tr} [\hat{P} e^{-S}] = \lim_{\zeta \rightarrow 0} Z_\zeta \langle \hat{Q} \rangle_\zeta, \quad (4)$$

where S is the (non-equilibrium) action, $Z_\zeta = \text{Tr}[e^{-S-\mu\hat{Q}}]$, and $\langle \dots \rangle_\zeta$ denotes the grand-canonical expectation value with respect to \hat{Q} . When projecting the expectation value of any physical operator acting on the molecule Hilbert space (e.g., b or σ^\pm) by inserting \hat{P} at the beginning of the Schwinger-Keldysh time contour [37], the prefactor \hat{Q} in \hat{P} can be dropped, because the physical operators annihilate the $\hat{Q} = 0$ auxiliary-particle sector by themselves (c.f. Eq. (1)). This means that even in a time-dependent non-equilibrium situation, the dynamics are constrained to the physical subspace $\hat{Q} = 1$ *exactly* by performing the auxiliary-field calculations in the grand-canonical ensemble with respect to \hat{Q} , where field-theoretic methods like Feynman diagrams are available, and taking the limit $\zeta \rightarrow 0$ at the end. This implies in turn that the Keldysh greater ($>$) and lesser ($<$) auxiliary propagators obey the following fugacity scaling laws in the limit $\zeta \rightarrow 0$,

$$\mathbf{G}^>(t, t') = \mathbf{G}_\zeta^>(t, t'), \quad \mathbf{G}^<(t, t') = \zeta \mathbf{G}_\zeta^<(t, t'), \quad (5)$$

where the subscript ζ denotes the grand-canonical propagator with respect to \hat{Q} . $\mathbf{G}^{\hat{\gg}}(t, t')$ stands for

the auxiliary propagators of the molecule electronic ground state, $[\mathbf{G}^>(t, t')]_{mn} = -i\langle d_{g, m}(t)d_{g, n}^\dagger(t')\rangle_{\zeta \rightarrow 0}$ and $[\mathbf{G}^<(t, t')]_{mn} = -i\langle d_{g, m}^\dagger(t')d_{g, n}(t)\rangle_{\zeta \rightarrow 0}$. The relations (5) arise because in $\mathbf{G}_\zeta^>(t, t')$ the factor ζ^{-1} cancels with the respective factor in the normalization $1/Z_{\hat{Q}=1}$ (c.f. Eq. 4), and $d_{g, m}$ annihilate the $\hat{Q} = 0$ subspace while $d_{g, m}^\dagger$ do not. The same scaling laws hold for the propagators of the electronic excited state, $[\mathbf{E}^>(t, t')]_{mn} = -i\langle d_{e, m}(t)d_{e, n}^\dagger(t')\rangle_{\zeta \rightarrow 0}$, $[\mathbf{E}^<(t, t')]_{mn} = -i\langle d_{e, m}^\dagger(t')d_{e, n}(t)\rangle_{\zeta \rightarrow 0}$. The projection of the molecule dynamics onto the physical $\hat{Q} = 1$ subspace is thus imposed exactly by the simple rule that in any auxiliary-particle Feynman diagram only terms of leading order in ζ are taken into account. In particular, the projected time-dependent Dyson equations for $\mathbf{G}^>(t, t')$ reduce to

$$\begin{aligned} (i\partial_t - \mathbf{h}_G) \mathbf{G}^<(t, t') &= \int_{t_0}^t d\bar{t} \Sigma_G^>(t, \bar{t}) \mathbf{G}^<(\bar{t}, t') \\ &\quad - \int_{t_0}^{t'} d\bar{t} \Sigma_G^<(t, \bar{t}) \mathbf{G}^>(\bar{t}, t'), \quad (6) \\ (i\partial_t - \mathbf{h}_G) \mathbf{G}^>(t, t') &= \int_{t'}^t d\bar{t} \Sigma_G^>(t, \bar{t}) \mathbf{G}^>(\bar{t}, t'), \end{aligned}$$

where \mathbf{h}_G is the non-interacting part of the Hamiltonian (2) in the electronic ground-state sector, t_0 denotes the beginning of the time evolution, and products of bold-faced quantities are understood as matrix products. Analogous equations hold for the excited-state propagators $\mathbf{E}^<(t, t')$. Observe how in the first of Eqs. (6), terms containing two pseudoparticle lesser functions have vanished, while in the second only terms without lesser functions remain.

The photon Green functions, defined as $[\mathbf{D}^>(t, t')]_{kk'} = -i\langle a_k(t)a_{k'}^\dagger(t')\rangle$, $[\mathbf{D}^<(t, t')]_{kk'} = -i\langle a_{k'}^\dagger(t')a_k(t)\rangle$, do not participate in the ζ scaling, since they do not operate in the molecule auxiliary-particle space. Thus, their Dyson equations have the usual form,

$$\begin{aligned} (i\partial_t - \mathbf{h}_D) \mathbf{D}^<(t, t') &= \int_{t_0}^t d\bar{t} [\Sigma_D^>(t, \bar{t}) - \Sigma_D^<(t, \bar{t})] \mathbf{D}^<(\bar{t}, t') \\ &\quad - \int_{t_0}^{t'} d\bar{t} \Sigma_D^<(t, \bar{t}) [\mathbf{D}^>(\bar{t}, t') - \mathbf{D}^<(\bar{t}, t')], \quad (7) \end{aligned}$$

where, according to the Jaynes-Cummings Hamiltonian H_{JC} , the photon self-energy is given by the irreducible part of the transverse physical electron propagator of a molecule, $\Sigma_D^<(t, t') = -ig^2\langle\sigma^-(t)\sigma^+(t')\rangle_{\text{irr}}^<$, with σ^\pm expressed by auxiliary bosons, Eq. (1). We also introduce the occupation of the photon ground mode as $N(t) = -\text{Im}D_{00}^<(t, t)$ with steady state $\bar{N} = \lim_{t \rightarrow \infty} N(t)$.

Conserving approximations – are necessary to implement the \hat{Q} conservation and can now be generated from

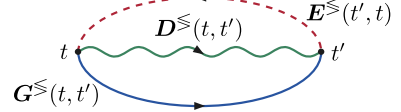


FIG. 2: Diagrammatic representation of the Luttinger-Ward functional generating the bosonic NCA self-energies.

a Luttinger-Ward functional [29, 38, 39]. In second self-consistent order in the molecule-photon coupling g , one obtains the analog of the non-crossing approximation (NCA), where the $\zeta \rightarrow 0$ self-energies read

$$\begin{aligned} \Sigma_G^>(t, t') &= ig^2 \mathbf{E}^>(t, t') \text{Tr} [\mathbf{D}^<(t', t)], \\ \Sigma_E^>(t, t') &= ig^2 \mathbf{G}^>(t, t') \text{Tr} [\mathbf{D}^<(t', t)], \\ \Sigma_D^>(t, t') &= ig^2 \zeta^{-1} \text{Tr} [\mathbf{E}^>(t, t') \mathbf{G}^<(t', t)], \end{aligned} \quad (8)$$

see Fig. 2. In the photon self-energy Σ_D , the factor ζ^{-1} stems from the global normalization factor $1/Z_{Q=1}$ (c.f. Eq. (4)) inherent to the physical electron propagator. In any self-energy insertion to $\mathbf{D}^<$ appearing in a pseudoparticle diagram, such a normalization is not present. Consequently, such insertions from the same molecule vanish by the projection $\zeta \rightarrow 0$.

For an arbitrary number of molecules M , the projection onto the physical subspace $\hat{Q} = 1$ is done as described above separately for each molecule m , since \hat{Q} is locally conserved on each molecule. Coherence between different molecules may nevertheless be mediated by the photon-mode coupling to all the molecules. For multiple molecules, the right-hand side of Eq. (7) acquires an additional prefactor M , and the photon propagators within self-energies for a molecule m (Fig. 2) are renormalized by self-energy contributions from other molecules $m' \neq m$.

Driven-dissipative photon-molecule dynamics. – While the molecule-bath dynamics are treated fully coherently, we incorporate the external drive and loss by adding Lindblad terms to the master equation for the density matrix, $\partial_t \rho = i[\rho, H] + \sum_k \kappa \mathcal{L}[a_k] \rho + \mathcal{L}_M \rho$, with $\mathcal{L}[X]\rho = X\rho X^\dagger - \{X^\dagger X, \rho\}/2$. The cavity loss is κ and $\mathcal{L}_M = \mathcal{L}_{\uparrow, \downarrow} + \mathcal{L}_{\text{relax}}$, where the external drive and radiationless decay of electron excitations are described by $\mathcal{L}_{\uparrow, \downarrow} = \sum_n \{\Gamma_\uparrow \mathcal{L}[d_{e, n}^\dagger d_{g, n}] + \Gamma_\downarrow \mathcal{L}[d_{g, n}^\dagger d_{e, n}]\}$ (c.f. Fig. 1 (b)), and phonon relaxation due to molecular solvent collisions by

$$\begin{aligned} \mathcal{L}_{\text{relax}} &= \sum_{n, \sigma} (n+1) \left(\lambda (\bar{n}(\Omega) + 1) \mathcal{L}[d_{\sigma, n}^\dagger d_{\sigma, n+1}] \right. \\ &\quad \left. + \lambda \bar{n}(\Omega) \mathcal{L}[d_{\sigma, n+1}^\dagger d_{\sigma, n}] \right). \end{aligned} \quad (9)$$

Here, λ is the relaxation rate of molecular vibrations, and the solvent temperature enters implicitly through the average phonon occupation number $\bar{n}(\Omega)$. See [36] for how this is formulated within the Schwinger-Keldysh non-equilibrium field theory used in the present work.

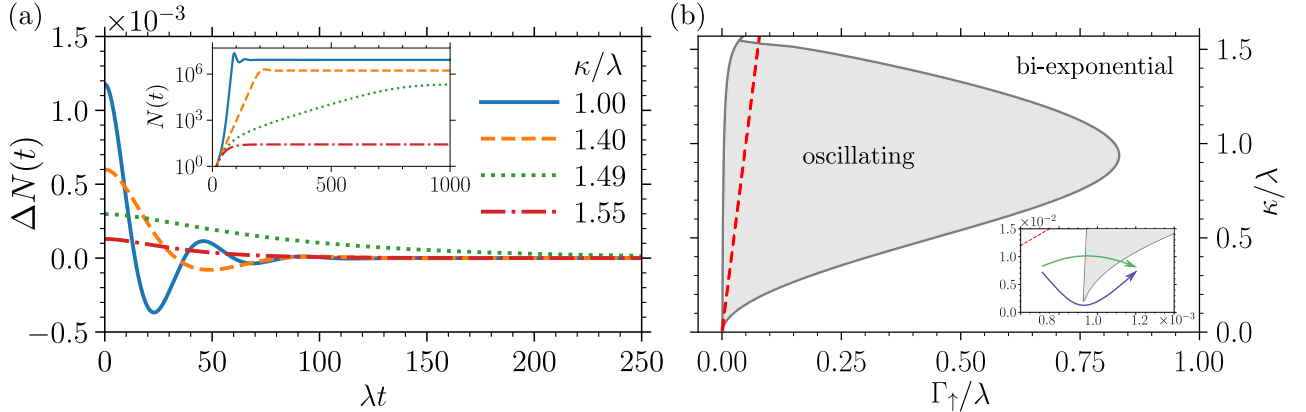


FIG. 3: (a) Photon relaxation $\Delta N(t) = N(t) - \bar{N}$ for initial conditions $N(0) = 0$, $iG_{00}^{<}(0, 0) = 1$, and $M = 10^9$, $g/\lambda = 4.5 \cdot 10^{-5}$, $\delta_0/\lambda = -1.00$, $\Omega/\lambda = 1.00$, $S = 1$, $\bar{n} = 0.25$, $\kappa/\Gamma_\uparrow = 20$, $\Gamma_\downarrow/\lambda = 1.25 \cdot 10^{-3}$, $\lambda\tau_{\text{mem}} = 4.0$, and time step $\lambda\Delta t = 2^{-4}$. For the low solvent temperature encoded by $\bar{n} = 0.25$, truncation of the phonon spectrum at $n_{\text{max}} = 4$ is appropriate. (b) Global phase diagram classifying $\Delta N(t)$, obtained from RE [36]. The boundary is marked by exceptional points in the relaxation spectrum. Red, dashed line: $\kappa/\Gamma_\uparrow = 20$. Inset: avoiding the transition by circumventing the critical point of the oscillatory phase.

Numerical results and discussion. – We solve the Kadanoff-Baym Eqs. (6), (7) self-consistently with Eq. (8) using a multi-step predictor-corrector method [40, 41] developed earlier to facilitate adaptive two-time evolution [42]. We truncate the time integrals in Eqs. (6) (7) at the memory time τ_{mem} , which is set by the inverse, dissipative relaxation rates κ, λ [36]. This allows for an efficient yet accurate simulation. For small system sizes, we find quantitative agreement with quasieexact numerical time evolution [16]. As a further consistency check, in the Markovian limit (phonon relaxation rate λ faster than any other scale in the system) our approach reduces to the previously studied semi-classical RE [17], with effective absorption and emission coefficients $\Gamma_k^\pm = \Gamma(\pm\delta_k) \equiv -2 \text{Re } K(\pm\delta_k)$, as derived in [36]. $\Gamma(\pm\delta_k)$ encodes the molecular absorption and emission spectra shown in Fig. 1(c), assuming k -independent detuning $\delta_k = \delta$. Around the zero-phonon line, $\delta = 0$, these spectra satisfy the Kennard-Stepanov relation at the temperature fixed implicitly via $\bar{n}(\Omega)$ (see parameter values in Fig. 3). For the numerical evaluations, we consider a low solvent temperature such that $\bar{n}(\Omega) = 0.25$ which justifies truncating the phonon occupation numbers at $n \leq n_{\text{max}} = 4$.

Previous experiments [11] revealed that driven-dissipative photon condensates possess hidden, non-trivial dynamics in the second-order coherence $g^{(2)}(t) = \lim_{T \rightarrow \infty} \langle N(T+t)N(T) \rangle / \langle N(T) \rangle^2$, despite the spectrally resolved photon number following an equilibrium Bose-Einstein distribution. The $g^{(2)}(t)$ oscillation frequency and decay rates as functions of Γ_\uparrow and κ , i.e. of the distance from true equilibrium, show a non-Hermitian phase transition marked by an exceptional point [11]. Deviations from this picture, obtained on the basis of the RE [12, 17], are to be expected when the system is strongly out of equilibrium. Our formalism is ideally suited for

studying such non-Markovian effects.

We start the time evolution with an empty single-mode cavity filled with an ensemble of molecules in the ground state and drive the system into a steady state by a constant optical pumping Γ_\uparrow (inset of Fig. 3(a)). Once stationarity is reached, a short Gaussian pulse is added (Eq. (S.30) of [36]) to trigger a response of the photon field as the system is slightly displaced from the steady state. Via quantum regression [43], the ensuing relaxation is then equivalent to the spontaneous intensity fluctuations described by $g^{(2)}(t)$. As shown in Fig. 3(a), the photon relaxation changes qualitatively from oscillatory to bi-exponential as a function of κ (observe that κ/Γ_\uparrow is kept fixed) [11, 12]. This behavior is generic and independent of the specific parameters chosen. For each set of parameters, the transition between the two behaviors is characterized by an exceptional point where the eigenvalues of the linearized regression dynamics [12] coalesce and switch from a pair of complex frequencies $\pm i\omega - \tau^{-1}$ to two real relaxation rates $\tau^{-1}, \tau'^{-1} > \tau^{-1}$ [44]. We extract these parameters by fitting the sum of two complex exponential functions to the numerical results [36].

We find that the phase boundary between both behaviors retraces qualitatively the one obtained from the RE model [36]. Therefore, in Fig. 3(b) we show the global dynamical phase diagram of the photon relaxation as a function of the drive Γ_\uparrow and dissipation κ as obtained from the RE, and compare in Fig. 4 the FQD, Eqs. (6)–(8), with the RE results along the red, dashed line shown in Fig. 3 (b). Evidently, the RE model agrees with the FQD only near equilibrium ($\kappa/\lambda \ll 1, \Gamma_\uparrow \ll 1$), while for strong drive and dissipation deviations occur, indicating a breakdown of the Markov assumption inherent to the RE approach: the system becomes non-Markovian in this stronger sense, as opposed to merely a frequency-

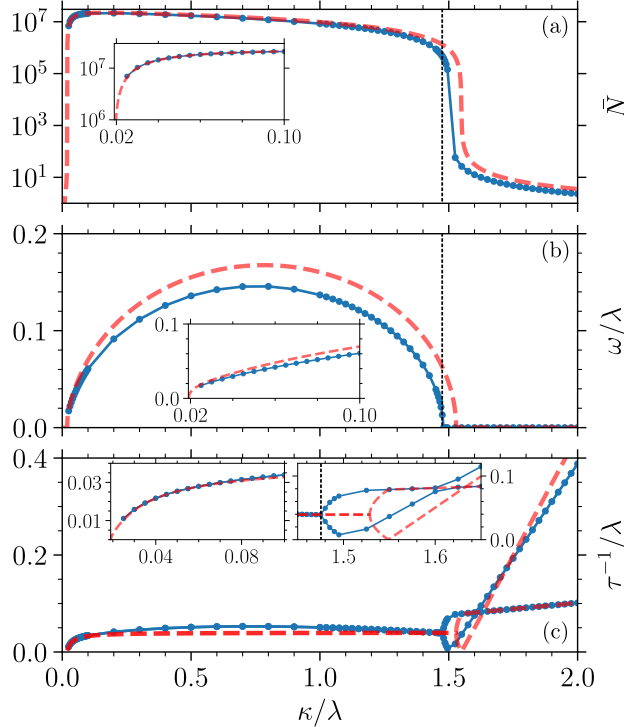


FIG. 4: Steady-state photon number \bar{N} , and relaxation frequency ω and rate τ^{-1} as functions of the cavity loss κ for $\kappa/\Gamma_\uparrow = 20 = \text{const}$. Blue, solid curves: FQD, Eqs. (6)-(8); red, dashed curves: RE model [36]. $\lambda\Gamma_0^- = g^2 \cdot 0.796$, $\Gamma_0^+/\Gamma_0^- = 0.741$ (obtained from Fig. (S1) of [36]). The vertical line marks the exceptional point.

dependent photo-molecular coupling [13]. As seen from Fig. 4 (a), the steady-state occupation \bar{N} collapses beyond a critical loss rate κ in spite of $\kappa/\Gamma_\uparrow = \text{const}$. [4]. This seemingly counterintuitive effect is due to the loss of coherence with increasing κ and Γ_\uparrow . This decondensation is accompanied by critical slowing down, i.e., a diverging relaxation time, $\tau^{-1} \rightarrow 0$ (Fig. 3 (c)), a clear sign of a non-equilibrium phase transition, while the fast relaxation rate τ' remains finite. Since $\tau^{-1} \rightarrow 0$ is only possible when both eigenvalues are real ($\omega = 0$) [12], the decondensation threshold must always occur in the bi-exponential phase, c.f. Fig. 4 (a), (b).

We furthermore notice that the strongly driven, non-equilibrium regime [upper right region in Fig. 3 (b)] represents a laser. That is, the near-equilibrium photon BEC phase is qualitatively separated from the laser phase by a hidden $g^{(2)}(t)$ transition, where this phase transition can be circumvented by the path in parameter space shown in the inset of Fig. 3 (b), in much the same sense as the liquid-vapor transition in water can be circumvented by going through a high-pressure state.

Conclusion. – We have introduced a non-equilibrium auxiliary field theory which faithfully describes the time-dependent quantum dynamics of general coupled system-

bath set-ups, here generalized to open, driven-dissipative quantum systems such as photon BECs coupled to dye-molecule reservoirs [1] or exciton-polariton systems [45]. Our method may also be applied to the full quantum dynamics of multiple qubits coupled to sources of non-Markovian noise [46].

For the open photon-BEC system, we find significant non-Markovian memory effects in the strongly driven regime where system loss κ and reservoir relaxation λ become comparable. We uncovered the global shape of the phase diagram partially explored in [11]. These calculations establish that the near-equilibrium photon BEC is separated from the lasing regime by a hidden phase transition of the photon density response.

We acknowledge useful discussions with Fahri E. Öztürk, Julian Schmitt, Michael Turaev, Frank Vewinger, and Martin Weitz. This work was supported in part by the Deutsche Forschungsgemeinschaft (DFG) within the Cooperative Research Center TRR 185 (277625399) and the Cluster of Excellence ML4Q (390534769).

* E-mail: t.bode@fz-juelich.de

† Email: kroha@physik.uni-bonn.de

- [1] J. Klaers, J. Schmitt, F. Vewinger, and M. Weitz, *Nature* **468**, 545 (2010).
- [2] J. Klaers, J. Schmitt, T. Damm, F. Vewinger, and M. Weitz, *Phys. Rev. Lett.* **108**, 160403 (2012).
- [3] J. Schmitt, T. Damm, D. Dung, F. Vewinger, J. Klaers, and M. Weitz, *Phys. Rev. Lett.* **112**, 030401 (2014).
- [4] H. J. Hesten, R. A. Nyman, and F. Mintert, *Phys. Rev. Lett.* **120**, 040601 (2018).
- [5] B. T. Walker, L. C. Flatten, H. J. Hesten, F. Mintert, D. Hunger, A. A. P. Trichet, J. M. Smith, and R. A. Nyman, *Nature Physics* **14**, 1173 (2018).
- [6] J. Keeling and S. Kéna-Cohen, *Annual Review of Physical Chemistry* **71**, 435 (2020), PMID: 32126177.
- [7] M. Ramezani, A. Halpin, S. Wang, M. Berghuis, and J. G. Rivas, *Nano Letters* **19**, 8590 (2019).
- [8] T. K. Hakala, A. J. Moilanen, A. I. Väkeväinen, R. Guo, J.-P. Martikainen, K. S. Daskalakis, H. T. Rekola, A. Julku, and P. Törmä, *Nature Physics* **14**, 739 (2018).
- [9] C. Clear, R. C. Schofield, K. D. Major, J. Iles-Smith, A. S. Clark, and D. P. S. McCutcheon, *Phys. Rev. Lett.* **124**, 153602 (2020).
- [10] L. M. Sieberer, M. Buchhold, and S. Diehl, *Reports on Progress in Physics* **79**, 096001 (2016).
- [11] F. E. Öztürk, T. Lappe, G. Hellmann, J. Schmitt, J. Klaers, F. Vewinger, J. Kroha, and M. Weitz, *Science* **372**, 88 (2021).
- [12] F. E. Öztürk, T. Lappe, G. Hellmann, J. Schmitt, J. Klaers, F. Vewinger, J. Kroha, and M. Weitz, *Phys. Rev. A* **100**, 043803 (2019).
- [13] J. Schmitt, *Journal of Physics B: Atomic, Molecular and Optical Physics* **51**, 173001 (2018).
- [14] C. Kurtscheid, D. Dung, E. Busley, F. Vewinger, A. Rosch, and M. Weitz, *Science* **366**, 894 (2019).

- [15] I. de Vega and D. Alonso, *Rev. Mod. Phys.* **89**, 015001 (2017).
- [16] J. del Pino, F. A. Y. N. Schröder, A. W. Chin, J. Feist, and F. J. Garcia-Vidal, *Phys. Rev. Lett.* **121**, 227401 (2018).
- [17] P. Kirton and J. Keeling, *Phys. Rev. Lett.* **111**, 100404 (2013).
- [18] P. Kirton and J. Keeling, *Phys. Rev. A* **91**, 033826 (2015).
- [19] J. Keeling and P. Kirton, *Phys. Rev. A* **93**, 013829 (2016).
- [20] M. Radonjić, W. Kopylov, A. Balaž, and A. Pelster, *New Journal of Physics* **20**, 055014 (2018).
- [21] M. Marthaler, Y. Utsumi, D. S. Golubev, A. Shnirman, and G. Schön, *Phys. Rev. Lett.* **107**, 093901 (2011).
- [22] J. Lebreuilly, A. Chiocchetta, and I. Carusotto, *Phys. Rev. A* **97**, 033603 (2018).
- [23] A. A. Abrikosov, *Physics Physique Fizika* **2**, 5 (1965).
- [24] S. E. Barnes, *Journal of Physics F: Metal Physics* **6**, 1375 (1976).
- [25] S. E. Barnes, *Journal of Physics F: Metal Physics* **7**, 2637 (1977).
- [26] N. E. Bickers, *Rev. Mod. Phys.* **59**, 845 (1987).
- [27] P. Coleman, *Phys. Rev. B* **29**, 3035 (1984).
- [28] J. Kroha and P. Wölfle, *Acta Phys. Pol. B* **29**, 3781 (1998).
- [29] J. Kroha and P. Wölfle, *J. Phys. Soc Jap.* **74**, 16 (2005).
- [30] P. W. Anderson, *Phys. Rev.* **124**, 41 (1961).
- [31] D. C. Langreth and P. Nordlander, *Phys. Rev. B* **43**, 2541 (1991).
- [32] N. S. Wingreen and Y. Meir, *Phys. Rev. B* **49**, 11040 (1994).
- [33] M. H. Hettler, J. Kroha, and S. Hershfield, *Phys. Rev. B* **58**, 5649 (1998).
- [34] J. Kroha and A. Zawadowski, *Phys. Rev. Lett.* **88**, 176803 (2002).
- [35] Eckstein, Martin and Werner, Philipp, *Phys. Rev. B* **82**, 115115 (2010).
- [36] See Supplemental Material at [URL will be inserted by publisher] for details of the calculations, which includes Refs. [10, 17, 18, 47].
- [37] A. Kamenev, *Field Theory of Non-Equilibrium Systems* (Cambridge University Press, 2023).
- [38] J. Berges, *AIP Conference Proceedings* **739**, 3 (2004).
- [39] T. Gasenzer, J. Berges, M. G. Schmidt, and M. Seco, *Phys. Rev. A* **72**, 063604 (2005).
- [40] S. Bock, A. Liliuashvili, and T. Gasenzer, *Phys. Rev. B* **94**, 045108 (2016).
- [41] A. Stan, N. E. Dahlen, and R. van Leeuwen, *The Journal of Chemical Physics* **130**, 224101 (2009).
- [42] F. Meirinhos, M. Kajan, J. Kroha, and T. Bode, *SciPost Phys. Core* **5**, 030 (2022).
- [43] H. J. Carmichael, *Statistical Methods in Quantum Optics 1: Master Equations and Fokker-Planck Equations* (Springer Berlin, Heidelberg, 2013).
- [44] W. D. Heiss, *Journal of Physics A: Mathematical and Theoretical* **45**, 444016 (2012).
- [45] J. Kasprzak, M. Richard, S. Kundermann, A. Baas, P. Jeaumbrun, J. M. J. Keeling, F. M. Marchetti, M. H. Szymańska, R. André, J. L. Staehli, V. Savona, P. B. Littlewood, B. Deveaud, and L. S. Dang, *Nature* **443**, 409 (2006).
- [46] G. A. L. White, C. D. Hill, F. A. Pollock, L. C. L. Hollenberg, and K. Modi, *Nature Communications* **11**, 6301 (2020).
- [47] J. Schwinger, *Journal of Mathematical Physics* **2**, 407 (1961).

Supplemental Material – Non-Markovian Dynamics of Open Quantum Gases

Tim Bode,^{1,2,*} Michael Kajan,¹ Francisco Meirinhos,¹ and Johann Kroha^{1,†}

¹*Physikalisches Institut and Bethe Center for Theoretical Physics,*

Universität Bonn, Nussallee 12, 53115 Bonn, Germany

²*Institute for Quantum Computing Analytics (PGI-12),*

Forschungszentrum Jülich, 52425 Jülich, Germany

1. Rate Equations

The rate equations for the photon and molecule number dynamics [17, 18] can be derived from the full quantum field theory under the semi-classical assumption that (in the frame rotating with the detuning δ_k) the photon Green functions are approximately constant over the support of the molecule memory integrals, which is determined by the phonon relaxation rate λ . The two-time photon Green functions obey the equations of motion (see Eq. (7) of the main text)

$$i\partial_t \mathbf{D}^{\lessgtr}(t, t') = M \int_{t_0}^t d\bar{t} [\Sigma_D^>(\bar{t}, t) - \Sigma_D^<(\bar{t}, t)] \mathbf{D}^{\lessgtr}(\bar{t}, t') - M \int_{t_0}^{t'} d\bar{t} \Sigma_D^{\lessgtr}(\bar{t}, t) [\mathbf{D}^>(\bar{t}, t') - \mathbf{D}^<(\bar{t}, t')] \quad (\text{S.1})$$

and

$$i\partial_{t'} \mathbf{D}^{\lessgtr}(t, t') = M \int_{t_0}^{t'} d\bar{t} [\Sigma_D^>(\bar{t}, t') - \Sigma_D^<(\bar{t}, t')] \mathbf{D}^{\lessgtr}(\bar{t}, t) - M \int_{t_0}^t d\bar{t} \Sigma_D^{\lessgtr}(\bar{t}, t') [\mathbf{D}^>(\bar{t}, t) - \mathbf{D}^<(\bar{t}, t)]. \quad (\text{S.2})$$

Adding these two, one obtains a symmetrized equation of motion in terms of the center-of-motion time $T = (t + t')/2$ in the equal-time limit $t = t'$,

$$i\partial_t \mathbf{D}^<(t, t) = M \int_{t_0}^t d\bar{t} [\Sigma_D^>(\bar{t}, t) \mathbf{D}^<(\bar{t}, t) - \Sigma_D^<(\bar{t}, t) \mathbf{D}^>(\bar{t}, t) + \mathbf{D}^<(\bar{t}, t) \Sigma_D^>(\bar{t}, t) - \mathbf{D}^>(\bar{t}, t) \Sigma_D^<(\bar{t}, t)]. \quad (\text{S.3})$$

Then we can write the equation of motion for the photon number $N_k(t) = iD_{kk}^<(t, t)$, including the Lindblad relaxation term due to cavity loss κ discussed in the main text and in section 2 below, as

$$i\partial_t D_{kk}^<(t, t) = -i\kappa D_{kk}^<(t, t) + iMg^2 \int_0^t d\bar{t} \left\{ \text{Tr} [\mathbf{E}^>(\bar{t}, t) \mathbf{G}^<(\bar{t}, t)] D_{kk}^<(\bar{t}, t) + \text{Tr} [\mathbf{G}^<(\bar{t}, t) \mathbf{E}^>(\bar{t}, t)] D_{kk}^<(\bar{t}, t) \right. \\ \left. - \text{Tr} [\mathbf{E}^<(\bar{t}, t) \mathbf{G}^>(\bar{t}, t)] D_{kk}^>(\bar{t}, t) - \text{Tr} [\mathbf{G}^>(\bar{t}, t) \mathbf{E}^<(\bar{t}, t)] D_{kk}^>(\bar{t}, t) \right\}, \quad (\text{S.4})$$

where we have absorbed the prefactor ζ^{-1} of Σ_D^{\lessgtr} and then dropped the subscripts ζ . Now, when the vibrational states have a rapid relaxation (i.e. are strongly broadened by collisions with the surrounding solvent), the dynamics of the pseudo-particles in relative time $(t - t')$ is approximately stationary and independent of the dynamics in forward time T . The vibrational states can then only have an overall forward evolution, which is to say that a quantum going either into the ground- or excited-state manifold will end up in vibrational state n with a fixed probability p_n , where $\sum_n p_n = 1$. This enables us to write, for instance,

$$\int_0^t d\bar{t} G_{nm}^<(\bar{t}, t) \approx G^<(t, t) \int_0^\infty d(t - \bar{t}) e^{i\omega_D(t - \bar{t})} e^{-(\Gamma_{\uparrow} + \Gamma_{\downarrow})(t - \bar{t})/2} g_{nm}(t - \bar{t}), \quad (\text{S.5})$$

where g_{nm} encodes the relative-time dynamics of $G_{nm}^<(t, t')$ beyond the effect of ω_D and $\Gamma_{\uparrow, \downarrow}$, that is, the vibrational frequencies and relaxation. It has the property $g_{nm}(0) = G_{nm}^<(t, t)/G^<(t, t)$, such that $g_{nn}(0) = p_n$. The analogous term for the excited states is

$$\int_0^t d\bar{t} E_{nm}^<(\bar{t}, t) \approx E^<(t, t) \int_0^\infty d(t - \bar{t}) e^{i\omega_D(t - \bar{t})} e^{-(\Gamma_{\uparrow} + \Gamma_{\downarrow})(t - \bar{t})/2} e_{nm}(t - \bar{t}), \quad (\text{S.6})$$

where similarly $e_{nm}(0) = E_{nm}^<(t, t)/E^<(t, t)$. We furthermore introduce the total number of excited molecules as

$$M_{\uparrow}(t) = iM \text{Tr} \mathbf{E}^<(t, t) = iM \sum_{n=0}^{\infty} E_{nn}^<(t, t) = iM E^<(t, t), \quad (\text{S.7})$$

and similarly for the ground state where

$$M - M_\uparrow(t) = iM \operatorname{Tr} \mathbf{G}^<(t, t) = iM \sum_{n=0}^{\infty} G_{nn}^<(t, t) = iMG^<(t, t), \quad (\text{S.8})$$

such that the constraint $\hat{Q} = 1$ ensures total number conservation. Finally, the above assumptions ensure that the greater functions do not possess a forward-time dependence, i.e.

$$\begin{aligned} E_{mn}^>(t, t') &\approx E_{mn}^>(t - t'), \\ G_{mn}^>(t, t') &\approx G_{mn}^>(t - t'). \end{aligned} \quad (\text{S.9})$$

With these definitions, and using that under the approximation described above one can pull out the photon propagators from the time integrals and normalise by the respective occupation number of the ground and the excited states, we may transform Eq. (S.4) into

$$\begin{aligned} \partial_t N_k(t) &= -\kappa N_k(t) - [K(+\delta_k) + K^*(-\delta_k)] N_k(t) (M - M_\uparrow(t)) \\ &\quad + [K^*(-\delta_k) + K(-\delta_k)] (N_k(t) + 1) M_\uparrow(t) \\ &= -\kappa N_k(t) - \Gamma_k^+ N_k(t) (M - M_\uparrow(t)) + \Gamma_k^- (N_k(t) + 1) M_\uparrow(t), \end{aligned} \quad (\text{S.10})$$

which is the established result [17, 18], and we have identified $\Gamma_k^\pm = \Gamma(\pm\delta_k) = 2 \operatorname{Re} K(\pm\delta_k)$. In our case, the emission and absorption coefficients are then given via

$$K(\delta) = g^2 \int_0^\infty d(t - \bar{t}) e^{i\delta(t - \bar{t})} e^{-(\Gamma_\uparrow + \Gamma_\downarrow)(t - \bar{t})/2} A(t - \bar{t}), \quad (\text{S.11})$$

where

$$A(\tau) = \sum_{m,n=0}^{\infty} iG_{mn}^>(\tau) e_{nm}(-\tau) = \sum_{m,n=0}^{\infty} iE_{mn}^>(\tau) g_{nm}(-\tau). \quad (\text{S.12})$$

This is to be compared with the original expression in the quantum master equation derived via the usual Born-Markov approximation [17, 18]:

$$K(\delta) = g^2 \int_0^\infty d(t - \bar{t}) e^{i\delta(t - \bar{t})} e^{-(\Gamma_\uparrow + \Gamma_\downarrow)(t - \bar{t})/2} f(t - \bar{t}), \quad (\text{S.13})$$

where $f(t)$ is the polaron correlation function. An alternative and more practical way of defining Eq. (S.11), which is also leading directly to Eq. (S.10), follows by letting

$$K(\delta) = ig^2 (\operatorname{Tr} \mathbf{G}^<(t, t))^{-1} \int_0^t dt \operatorname{Tr} [\mathbf{E}^>(t, \bar{t}) \mathbf{G}^<(\bar{t}, t)] = ig^2 (\operatorname{Tr} \mathbf{E}^<(t, t))^{-1} \int_0^t dt \operatorname{Tr} [\mathbf{E}^<(t, \bar{t}) \mathbf{G}^>(\bar{t}, t)]. \quad (\text{S.14})$$

Defining $K(\delta)$ in *this* way occurs with the thought in mind that it is effectively the right-hand sides of Eq. (S.14) acting instead of their previous definitions [17, 18] when parameters are chosen such that the pseudo-particle dynamics effectively recovers the rate equations. Finally, the molecular rate equation follows completely analogously and reads

$$\partial_t M_\uparrow(t) = \Gamma_\uparrow (M - M_\uparrow(t)) - \Gamma_\downarrow M_\uparrow(t) + \sum_k [\Gamma_k^+ N_k(t) (M - M_\uparrow(t)) - \Gamma_k^- (N_k(t) + 1) M_\uparrow(t)]. \quad (\text{S.15})$$

2. Driven-Dissipative Processes in Schwinger-Keldysh Formalism

As the simplest example, consider a cavity mode of frequency ω_0 , coupled to an environment at a low temperature such that $\hbar\omega_0 \gg \beta^{-1}$, is described by the Lindblad master equation

$$\partial_t \hat{\rho} = -i [\hat{H}\hat{\rho} - \hat{\rho}\hat{H}^\dagger] + \kappa a \hat{\rho} a^\dagger, \quad (\text{S.16})$$

with the non-Hermitian Hamiltonian

$$\hat{H} = (\omega_0 - i\kappa/2) a^\dagger a. \quad (\text{S.17})$$

In its most general formulation as given by Schwinger [47], the formalism easily captures this kind of dynamics. The Schwinger action that appears in the coherent-state expansion of the non-equilibrium partition function Z is [10]

$$S[\phi_\pm^*, \phi_\pm] = \int dt [\phi_+^* (i\partial_t - \omega_0 + i\kappa/2) \phi_+ - \phi_-^* (i\partial_t - \omega_0 - i\kappa/2) \phi_- - i\kappa \phi_+ \phi_-^*]. \quad (\text{S.18})$$

Note how this contains a contribution across the two branches of the contour. The respective equations of motion for the greater and lesser Green functions are then

$$\begin{aligned} 0 &= (i\partial_t - \omega_0 + i\kappa/2) D^<(t, t'), \\ 0 &= (i\partial_t - \omega_0 - i\kappa/2) D^>(t, t') + i\kappa D^T(t, t'), \end{aligned} \quad (\text{S.19})$$

where now the time-ordered Green function appears explicitly. The anti-time-ordered Green function would appear, for instance, when coupling to a bath at finite temperature. In the equal-time limit, these equations become

$$\begin{aligned} \partial_t D^<(t, t) &= -\kappa D^<(t, t), \\ \partial_t D^>(t, t) &= \kappa D^>(t, t) - \kappa [D^T(t, t) + D^{\bar{T}}(t, t)] \\ &= \kappa D^>(t, t) - \kappa [D^>(t, t) + D^<(t, t)], \end{aligned} \quad (\text{S.20})$$

which serves to illustrate how the commutator is preserved over time by the quantum jumps.

To have a consistent diagrammatic expansion for the four vertices g , $\Gamma_{\uparrow, \downarrow}$ and λ of our theory, we expand the corresponding vertices to second order in \hbar . For the incoherent couplings, such a two-loop expansion amounts to working in Hartree-Fock approximation.

The Lindblad operator describing the relaxation of the vibrational states,

$$\mathcal{L}_{\text{relax}} = \sum_{n, \sigma} (n + 1) \left(\lambda (\bar{n}(\Omega) + 1) \mathcal{L}[d_{\sigma, n}^\dagger d_{\sigma, n+1}] + \lambda \bar{n}(\Omega) \mathcal{L}[d_{\sigma, n+1}^\dagger d_{\sigma, n}] \right), \quad (\text{S.21})$$

can be understood by investigating the structurally equivalent operator

$$\frac{\Gamma}{2} \left[(\bar{n} + 1) \mathcal{L}[d_0^\dagger d_1] + \bar{n} \mathcal{L}[d_1^\dagger d_0] \right] \rho, \quad (\text{S.22})$$

where Γ is now an arbitrary constant. The projection is again performed by removing all terms with too many lesser functions, where one should keep in mind that for pseudo particles there holds

$$\mathbf{G}^>(T, 0) = \begin{pmatrix} G_{00}^>(T, 0) & G_{01}^>(T, 0) \\ G_{10}^>(T, 0) & G_{11}^>(T, 0) \end{pmatrix} = \begin{pmatrix} -i & 0 \\ 0 & -i \end{pmatrix} \quad (\text{S.23})$$

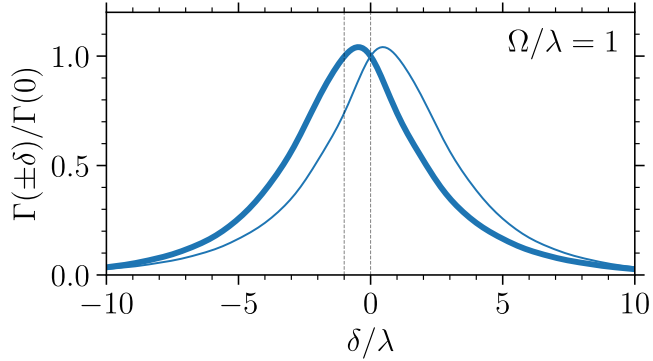


FIG. S1: Steady-state emission and absorption spectra $\Gamma^\pm(\delta)$ as calculated from the steady-state photon T -matrix for initial conditions $i\text{Tr} \mathbf{G}^<(0, 0) = i\text{Tr} \mathbf{E}^<(0, 0) = 1/2$, parameters $S = 1.00$, $\bar{n} = 0.25$, $\Gamma_\uparrow = \Gamma_\downarrow = 0$, vibrational-state truncation at $n = 4$, and $\lambda\Gamma(0) = g^2 \cdot 0.798$. The thick line corresponds to the emission coefficient $\Gamma(-\delta)$. Simulations calculated for 2^{11} steps up to a final time of $\lambda T_{\text{max}} = 16$ with memory time $\lambda\tau_{\text{mem}} = 4.0$ ($n_{\text{mem}} = 512$).

for all times T . We arrive at

$$\begin{aligned} i\partial_t \mathbf{G}^<(t, t') &= \mathbf{h}_G \mathbf{G}^<(t, t') + \frac{\Gamma \bar{n}}{2} \begin{pmatrix} G_{11}^>(t, t) & 0 \\ 0 & G_{00}^>(t, t) \end{pmatrix} \mathbf{G}^<(t, t') \\ &+ \frac{\Gamma}{2} \begin{pmatrix} 0 & 0 \\ 0 & G_{00}^>(t, t) \end{pmatrix} \mathbf{G}^<(t, t'), \end{aligned} \quad (\text{S.24a})$$

$$\begin{aligned} i\partial_t \mathbf{G}^>(t, t') &= \mathbf{h}_G \mathbf{G}^>(t, t') + \frac{\Gamma \bar{n}}{2} \begin{pmatrix} G_{11}^>(t, t) & 0 \\ 0 & G_{00}^>(t, t) \end{pmatrix} \mathbf{G}^>(t, t') \\ &+ \frac{\Gamma}{2} \begin{pmatrix} 0 & 0 \\ 0 & G_{00}^>(t, t) \end{pmatrix} \mathbf{G}^>(t, t'). \end{aligned} \quad (\text{S.24b})$$

These equations evidently possess the correct fugacity scalings. For the equal-time equation of $\mathbf{G}^<$, once more we remove all terms with the wrong scaling. This yields

$$\begin{aligned} i\dot{\mathbf{G}}^<(T, 0) &= [\mathbf{h}_G, \mathbf{G}^<(T, 0)] + \frac{\Gamma}{2} \left\{ \begin{pmatrix} \bar{n} G_{11}^>(T, 0) & 0 \\ 0 & (\bar{n} + 1) G_{00}^>(T, 0) \end{pmatrix}, \mathbf{G}^<(T, 0) \right\} \\ &- \Gamma \begin{pmatrix} (\bar{n} + 1) G_{11}^<(T, 0) & 0 \\ 0 & \bar{n} G_{00}^<(T, 0) \end{pmatrix} \mathbf{G}^>(T, 0), \end{aligned} \quad (\text{S.25})$$

where we have introduced an anti-commutator. Again, this equation has the correct fugacity scaling. As mentioned above, we do not need an equation for the equal-time evolution of $\mathbf{G}^>$. Within both the ground- and excited-state manifolds, the Lindblad operators of Eq. (S.21) couple neighboring vibrational states according to a structure which for the self-energy matrices of Eqs. (S.24) and $n + 1$ states in total looks like

$$(\bar{n} + 1) \text{diag}(0, G_{00}^>, 2G_{11}^>, \dots, nG_{n-1, n-1}^>) + \bar{n} \text{diag}(G_{11}^>, 2G_{22}^>, \dots, nG_{nn}^>, 0). \quad (\text{S.26})$$

We still have to consider the external pumping and electronic loss terms

$$\mathcal{L}_{\uparrow, \downarrow} = \sum_n \{ \Gamma_{\uparrow} \mathcal{L}[d_{e, n}^{\dagger} d_{g, n}] + \Gamma_{\downarrow} \mathcal{L}[d_{g, n}^{\dagger} d_{e, n}] \}.$$

The relevant matrices for this read

$$\begin{pmatrix} \mathbf{E}^{\leq}(t, t') & \mathbf{0} \\ \mathbf{0} & \mathbf{G}^{\leq}(t, t') \end{pmatrix}. \quad (\text{S.27})$$

In terms of these matrices, the contribution to the equations of motion can be written rather compactly as

$$i\partial_t \begin{pmatrix} \mathbf{E}^{\leq}(t, t') & \mathbf{0} \\ \mathbf{0} & \mathbf{G}^{\leq}(t, t') \end{pmatrix} = \frac{\Gamma_{\uparrow}}{2} \begin{pmatrix} \mathbf{0} & \mathbf{0} \\ \mathbf{0} & \text{diag}(\mathbf{E}^>(t, t)) \end{pmatrix} \begin{pmatrix} \mathbf{E}^{\leq}(t, t') & \mathbf{0} \\ \mathbf{0} & \mathbf{G}^{\leq}(t, t') \end{pmatrix}. \quad (\text{S.28})$$

For the forward dynamics, we find

$$\begin{aligned} i \begin{pmatrix} \dot{\mathbf{E}}^<(T, 0) & \mathbf{0} \\ \mathbf{0} & \dot{\mathbf{G}}^<(T, 0) \end{pmatrix} &= \frac{\Gamma_{\uparrow}}{2} \left\{ \begin{pmatrix} \mathbf{0} & \mathbf{0} \\ \mathbf{0} & \text{diag}(\mathbf{E}^>(T, 0)) \end{pmatrix}, \begin{pmatrix} \mathbf{E}^<(T, 0) & \mathbf{0} \\ \mathbf{0} & \mathbf{G}^<(T, 0) \end{pmatrix} \right\} \\ &- \Gamma_{\uparrow} \begin{pmatrix} \text{diag}(\mathbf{G}^<(T, 0)) & \mathbf{0} \\ \mathbf{0} & \mathbf{0} \end{pmatrix} \begin{pmatrix} \mathbf{E}^>(T, 0) & \mathbf{0} \\ \mathbf{0} & \mathbf{G}^>(T, 0) \end{pmatrix}. \end{aligned} \quad (\text{S.29})$$

The equations for the electronic loss Γ_{\downarrow} follow analogously. The functional form of the total external pumping reads

$$\Gamma_{\uparrow}(t) = \Gamma_{\uparrow} \left(1 + A \exp \left\{ -\frac{(t - t_P)^2}{2\sigma_P^2} \right\} \right), \quad (\text{S.30})$$

where t_P varies with the attainment of the steady state, and $A = 10^{-2}$, $\lambda\sigma_P = 1/2$. The initial conditions are $D^<(0, 0) = 0$, where we dropped the subscript $k = 0$ and $D^>(0, 0)$ follows from the commutator, $G_{mn}^<(0, 0) = -i\delta_{00}$ and $E_{mn}^<(0, 0) = 0$. The greater functions $G_{mn}^>(0, 0) = E_{mn}^>(0, 0) = -i\delta_{mn}$ are fixed by the projection.

Before concluding this section, consider Fig. S2 which shows the relaxation of the vibrational degrees of freedom in the electronic excited state induced by the vibrational relaxation in Eq. (S.21). The dashed line indicates the statistical average $-\text{Im} \sum_n n E_{nn}^<(t, t)$ which correctly approaches \bar{n} . We therefore conclude that our master equation is capable of describing the phonon thermalization adequately.

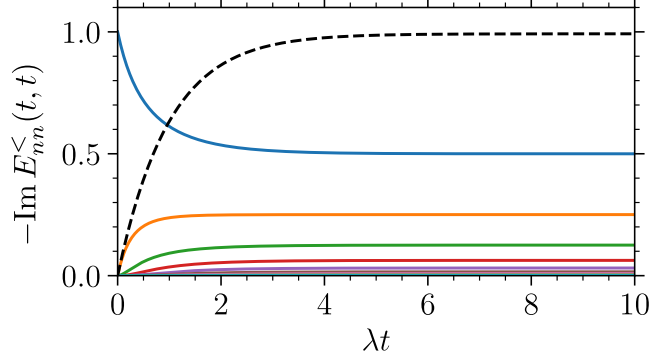


FIG. S2: Relaxation of the vibrational degrees of freedom in the electronic excited state. The dashed line shows $-\text{Im} \sum_{n=0}^{p_{\max}} n E_{nn}^{<}(t, t) \rightarrow \bar{n}$. The parameters are $g = 0$, i.e. we have decoupled the excited states from the rest of the system, $\omega_D/\lambda = 2.0$, $\Omega/\lambda = 0.1$, $S = 0.5$, $\bar{n} = 1.0$, $\Gamma_\uparrow = \Gamma_\downarrow = 0$. The initial conditions is $iE_{00}^{<}(0, 0) = 1$ with all other lesser functions being zero. The number of vibrational states considered is 10, which is equivalent to a maximal number of phonons $p_{\max} = 9$. The results were calculated with a step size of $10\lambda \cdot 2^{-9}$ for a number of 2^9 steps.

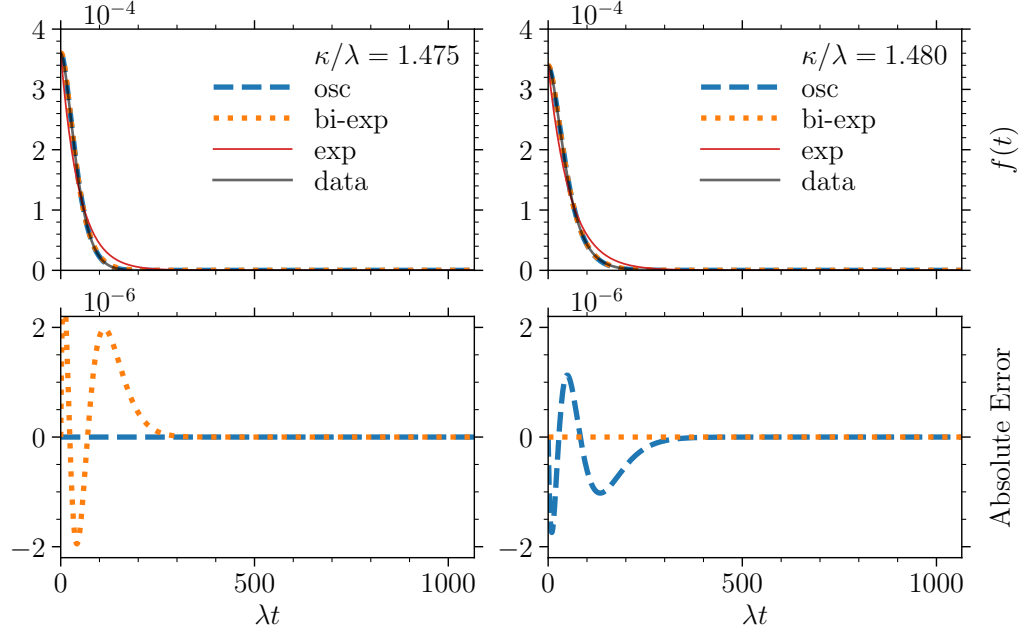


FIG. S3: Comparison of the fits directly to the left and right of the transition at large κ . Upper panels: Data and best fits for several different ansatz functions. A uni-exponential decay is also fitted to underline that it is not a possible best fit, as can indeed be judged by eye. Lower panels: The absolute error (difference of data and fit) for the two viable options f_{osc} and $f_{\text{bi-exp}}$.

3. Determining the Oscillation Frequency and Decay Rates of the Second-Order Correlations

The density responses in the main panel of Fig. 3 (a) show the evolution of $iD^{<}(t, t)$ following the Gaussian pulse (S.30), where the point $t = 0$ of the plot corresponds to the maximum of the curve after the Gaussian pulse has been injected. The frequency ω and decay rate τ in the oscillatory phase and the decay rates τ_1, τ_2 are extracted by least-squares fitting the functions

$$f_{\text{osc}}(t) = e^{-t/\tau} (f(0) \cos \omega t + C \sin \omega t),$$

$$f_{\text{bi-exp}}(t) = \frac{f(0)}{2} \left(e^{-t/\tau_1} + e^{-t/\tau_2} \right) + \frac{C}{2} \left(e^{-t/\tau_1} - e^{-t/\tau_2} \right) \quad (\text{S.31})$$

κ/λ	$s(\tau)$	$s(\omega)$	$s(C)$
1.475	$1.01 \cdot 10^{-8}$	$1.08 \cdot 10^{-8}$	$1.29 \cdot 10^{-9}$
1.480	$2.35 \cdot 10^{-5}$	$1.18 \cdot 10^{-3}$	$1.61 \cdot 10^{-1}$

TABLE I: Standard errors for the damped-oscillating ansatz.

κ/λ	$s(\tau_1)$	$s(\tau_2)$	$s(C)$
1.475	$2.84 \cdot 10^{-3}$	$2.93 \cdot 10^{-3}$	$2.85 \cdot 10^{-1}$
1.480	$4.02 \cdot 10^{-9}$	$1.45 \cdot 10^{-8}$	$4.42 \cdot 10^{-10}$

TABLE II: Standard errors for the bi-exponentially decaying ansatz.

to the numerical density responses. The quality of the fit is then estimated by the standard error, and the oscillatory or bi-exponential fit is accepted, whichever has the smaller error. This determines whether the response is classified as oscillating or bi-exponentially relaxing. An illustration of the fitting procedure is given in Fig. S3 and Tabs. I, II. One can see that even for these two points directly next to the transition, the fit classification is always unique.

4. Memory Truncation

Solving the equations of motion for interacting systems numerically on the two-time grid becomes computationally expansive when the number of grid points needs to be large. This happens whenever the product of the fastest system frequency and the required final time is not small. Any integral over relatively fast decaying Green functions, however, will be computable at sufficient precision over a small support that does not grow as the two-time grid expands towards its final size. In the same spirit, computing points far off the “time diagonal” $t = t'$ will be superfluous because they are negligible. In this way, by truncating the number of steps one moves away from the time diagonal, and by restricting the computation of the integrals to that same narrow “band”, it is indeed possible to achieve a quasi-linear scaling in the number of grid points without losing accuracy.

The quantitative consequences of different truncation parameters n_{mem} are studied in Fig. S4. Note that technically, n_{mem} is *not* the number of points included away from the diagonal moving in the direction $(t - t')$, but rather moving in the vertical and horizontal directions t and t' . A short-valued memory $n_{\text{mem}} = 24$ results in a certain number of points inaccurately remaining zero. With a longer-valued memory $n_{\text{mem}} = 64$, these points attain their proper values. However, looking to Fig. S4, we see that the influence of this is not considerable.

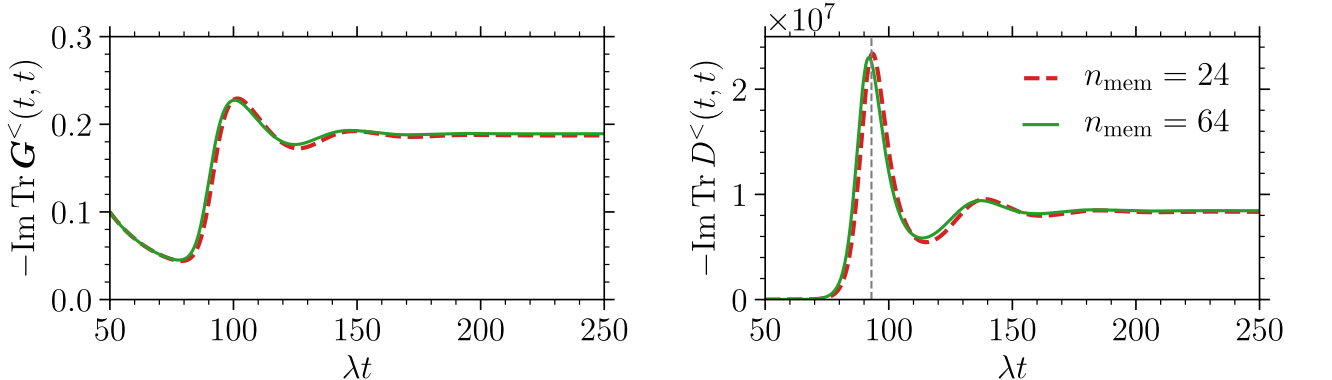


FIG. S4: Forward dynamics of a single photon mode $k = 0$ for different memory truncations. Initial conditions and parameters are $\text{Tr } D^<(0,0) = 0$, $iG_{00}^<(0,0) = 1$, and $M = 10^9$, $g/\lambda = 4.5 \cdot 10^{-5}$, $\omega_0/\lambda = -1.0$, $\kappa/\lambda = 1.0$, $\Omega/\lambda = 1.0$, $S = 1.0$, $\bar{n} = 0.25$, $\Gamma_\uparrow/\lambda = 0.05$, $\Gamma_\downarrow = \Gamma_\uparrow/40$, and vibrational-state truncation at $n = 4$. Simulations computed for 2^{13} steps up to a final time $\lambda T_{\text{max}} = 512$ with memory times $\lambda t_{\text{mem}} = \{1.5, 4.0\}$. The steady-state occupations are $\lim_{t \rightarrow \infty} i\text{Tr } D^<(t, t) = \{8.347 \cdot 10^6, 8.446 \cdot 10^6\}$, which means that the short-memory value deviates only by about 0.012.

* E-mail: t.bode@fz-juelich.de

† Email: kroha@physik.uni-bonn.de

- [1] J. Klaers, J. Schmitt, F. Vewinger, and M. Weitz, *Nature* **468**, 545 (2010).
- [2] J. Klaers, J. Schmitt, T. Damm, F. Vewinger, and M. Weitz, *Phys. Rev. Lett.* **108**, 160403 (2012).
- [3] J. Schmitt, T. Damm, D. Dung, F. Vewinger, J. Klaers, and M. Weitz, *Phys. Rev. Lett.* **112**, 030401 (2014).
- [4] H. J. Hesten, R. A. Nyman, and F. Mintert, *Phys. Rev. Lett.* **120**, 040601 (2018).
- [5] B. T. Walker, L. C. Flatten, H. J. Hesten, F. Mintert, D. Hunger, A. A. P. Trichet, J. M. Smith, and R. A. Nyman, *Nature Physics* **14**, 1173 (2018).
- [6] J. Keeling and S. Kéna-Cohen, *Annual Review of Physical Chemistry* **71**, 435 (2020), pMID: 32126177.
- [7] M. Ramezani, A. Halpin, S. Wang, M. Berghuis, and J. G. Rivas, *Nano Letters* **19**, 8590 (2019).
- [8] T. K. Hakala, A. J. Moilanen, A. I. Väkeväinen, R. Guo, J.-P. Martikainen, K. S. Daskalakis, H. T. Rekola, A. Julku, and P. Törmä, *Nature Physics* **14**, 739 (2018).
- [9] C. Clear, R. C. Schofield, K. D. Major, J. Iles-Smith, A. S. Clark, and D. P. S. McCutcheon, *Phys. Rev. Lett.* **124**, 153602 (2020).
- [10] L. M. Sieberer, M. Buchhold, and S. Diehl, *Reports on Progress in Physics* **79**, 096001 (2016).
- [11] F. E. Öztürk, T. Lappe, G. Hellmann, J. Schmitt, J. Klaers, F. Vewinger, J. Kroha, and M. Weitz, *Science* **372**, 88 (2021).
- [12] F. E. Ozturk, T. Lappe, G. Hellmann, J. Schmitt, J. Klaers, F. Vewinger, J. Kroha, and M. Weitz, *Phys. Rev. A* **100**, 043803 (2019).
- [13] J. Schmitt, *Journal of Physics B: Atomic, Molecular and Optical Physics* **51**, 173001 (2018).
- [14] C. Kurtscheid, D. Dung, E. Busley, F. Vewinger, A. Rosch, and M. Weitz, *Science* **366**, 894 (2019).
- [15] I. de Vega and D. Alonso, *Rev. Mod. Phys.* **89**, 015001 (2017).
- [16] J. del Pino, F. A. Y. N. Schröder, A. W. Chin, J. Feist, and F. J. Garcia-Vidal, *Phys. Rev. Lett.* **121**, 227401 (2018).
- [17] P. Kirton and J. Keeling, *Phys. Rev. Lett.* **111**, 100404 (2013).
- [18] P. Kirton and J. Keeling, *Phys. Rev. A* **91**, 033826 (2015).
- [19] J. Keeling and P. Kirton, *Phys. Rev. A* **93**, 013829 (2016).
- [20] M. Radonjić, W. Kopylov, A. Balaz, and A. Pelster, *New Journal of Physics* **20**, 055014 (2018).
- [21] M. Marthaler, Y. Utsumi, D. S. Golubev, A. Shnirman, and G. Schön, *Phys. Rev. Lett.* **107**, 093901 (2011).
- [22] J. Lebreuilly, A. Chiocchetta, and I. Carusotto, *Phys. Rev. A* **97**, 033603 (2018).
- [23] A. A. Abrikosov, *Physics Physique Fizika* **2**, 5 (1965).
- [24] S. E. Barnes, *Journal of Physics F: Metal Physics* **6**, 1375 (1976).
- [25] S. E. Barnes, *Journal of Physics F: Metal Physics* **7**, 2637 (1977).
- [26] N. E. Bickers, *Rev. Mod. Phys.* **59**, 845 (1987).
- [27] P. Coleman, *Phys. Rev. B* **29**, 3035 (1984).
- [28] J. Kroha and P. Wölfle, *Acta Phys. Pol. B* **29**, 3781 (1998).
- [29] J. Kroha and P. Wölfle, *J. Phys. Soc Jap.* **74**, 16 (2005).
- [30] P. W. Anderson, *Phys. Rev.* **124**, 41 (1961).
- [31] D. C. Langreth and P. Nordlander, *Phys. Rev. B* **43**, 2541 (1991).
- [32] N. S. Wingreen and Y. Meir, *Phys. Rev. B* **49**, 11040 (1994).
- [33] M. H. Hettler, J. Kroha, and S. Hershfield, *Phys. Rev. B* **58**, 5649 (1998).
- [34] J. Kroha and A. Zawadowski, *Phys. Rev. Lett.* **88**, 176803 (2002).
- [35] Eckstein, Martin and Werner, Philipp, *Phys. Rev. B* **82**, 115115 (2010).
- [36] See Supplemental Material at [URL will be inserted by publisher] for details of the calculations, which includes Refs. [10, 17, 18, 47].
- [37] A. Kamenev, *Field Theory of Non-Equilibrium Systems* (Cambridge University Press, 2023).
- [38] J. Berges, *AIP Conference Proceedings* **739**, 3 (2004).
- [39] T. Gasenzer, J. Berges, M. G. Schmidt, and M. Seco, *Phys. Rev. A* **72**, 063604 (2005).
- [40] S. Bock, A. Liliuashvili, and T. Gasenzer, *Phys. Rev. B* **94**, 045108 (2016).
- [41] A. Stan, N. E. Dahlen, and R. van Leeuwen, *The Journal of Chemical Physics* **130**, 224101 (2009).
- [42] F. Meirinhos, M. Kajan, J. Kroha, and T. Bode, *SciPost Phys. Core* **5**, 030 (2022).
- [43] H. J. Carmichael, *Statistical Methods in Quantum Optics 1: Master Equations and Fokker-Planck Equations* (Springer Berlin, Heidelberg, 2013).
- [44] W. D. Heiss, *Journal of Physics A: Mathematical and Theoretical* **45**, 444016 (2012).
- [45] J. Kasprzak, M. Richard, S. Kundermann, A. Baas, P. Jeambrun, J. M. J. Keeling, F. M. Marchetti, M. H. Szymańska, R. André, J. L. Staehli, V. Savona, P. B. Littlewood, B. Deveaud, and L. S. Dang, *Nature* **443**, 409 (2006).
- [46] G. A. L. White, C. D. Hill, F. A. Pollock, L. C. L. Hollenberg, and K. Modi, *Nature Communications* **11**, 6301 (2020).
- [47] J. Schwinger, *Journal of Mathematical Physics* **2**, 407 (1961).